

Obtaining data for the calculation of dihedral ϕ angles formed between pairs of crystalline planes in single-phase materials

Roniere Leite Soares ¹, Walman Benício de Castro ², Jackson de Brito Simões ³, Raiff Leite Soares ⁴

Adjunct Professor, Department of Production Engineering, Federal University of Campina Grande (UFCG), Teacher and researcher, City: Campina Grande, State of Paraíba, Country: Brazil¹

Titular Professor, Department of Mechanical Engineering, Federal University of Campina Grande (UFCG), Teacher and researcher, City: Campina Grande, State of Paraíba, Country: Brazil²

Adjunct Professor, Department of Mechanical Engineering, Federal Rural University of the Semiárid (UFERSA), Teacher and researcher, City: Caráúbas, State of Paraíba, Country: Brazil³

Orthopedist Surgeon, Traumatology Specialist, Federal University of Campina Grande (UFCG), Writer and researcher, City: Campina Grande, State of Paraíba, Country: Brazil⁴

ABSTRACT: The present article describes a methodology with which it is possible to discriminate the crystalline structure of the chemical element $_{13}\text{Al}$ as a way of demonstrating how it is possible to collect, catalog, visually represent, compile and integrate, through cataloged .CIF files, the main geometric characteristics of a crystalline cell as well as, after a detailed three-dimensional visualization, calculate the dihedral ϕ angle formed by the intersection between indexed crystalline planes. Aluminum was chosen because it is a very popular material in the metal-mechanical industry, resistant to oxidation, light, ductile and widely used in everyday life. The standard aluminum diffractogram was used as a starting point to identify the X-ray diffraction peaks that characterize the single phase that occurs at various 2Θ angles and under various percentage intensities. Finally, the 11 dihedral angles calculated using the equation adopted for this purpose were tabulated. The results are presented and discussed.

KEYWORDS: interplanar angle; dihedral angle; interaxial angle; phi angle; dihedral.

I. INTRODUCTION

Crystallography has driven interest not only in mathematics [1], solid state physics, materials science and engineering or chemical engineering, but also in various fields of graphic expression and drawing, specially geometric design, descriptive geometry and technical drawing. Nowadays, it is common for design professionals to be interested in the same subject, especially regarding the study of spatial organization of atoms and three-dimensional structures associated Bravais systems [2]. At the same time, the systematic use of computer programs dedicated to the crystallographic sciences has provided countless ways to interpret data and present it with more precision, dynamism and finishing. The Cambridge Structural Database (CSDS), for example, is a powerful suit of software that maintains information on nearly 700,000 crystal structures and various access modules for students and researchers [3]. In Brazil, the access to the DOT.LIB Crystalline Structures Database allows the handling of some online tools such as WebCSD, ConQuest, Mercury, Mogul, IsoStar and Hermes. Each one of these applications has a purpose that, in addition to the other typical features, complement each other. The latest version of Mercury (4.3.0) allows, from any CIF (Crystallographic Information File) [4], to calculate Bragg positions (degree) [5], intensities (cps), atomic positions (x y z), Miller indices (h k l) [6] and the interplanar distance (d , Å), in addition to other features. There are also free software that further enhance the acquisition of crystallographic data such as: VESTA format .vesta (Visualization for Electronic and Structural Analysis) [7], American Mineralogist Crystal Structure Database (*.amc) [8], CrystalMaker text file (*.cmt) [9], MINCRYST (Crystallographic Database for Minerals) [10], Draw XTL [11], CrysX-3D Viewer [12], Diamond [13][14] and Chem3D (*.cc1) [15], among others. However, there are certain structural characteristics that are still calculated manually, as they have not been included in such software until now. One of these characteristics is the interplanar angle [ϕ , °], which is the smallest aperture between a crystallographic plane and the subsequent one. It will always be an acute angle ($\phi < 90^\circ$). However, it can be classified into two types according to the aperture: sharp ($90^\circ >$

$\phi > 45^\circ$) and very sharp ($90^\circ > \phi < 45^\circ$). This *Phi* angle can also be synthesized as the point projection of the straight-intersection \overline{AB} , which belongs to the pair of planes considered, as shown in Figure 1(a). Figure 1(b) shows the congruence of the ϕ angles opposed by the vertex, equal to 54.73° , as well as Figure 1(c) shows the corresponding values. In this case, the value of the angle considered is classified as acute, that is, $90^\circ > \phi > 45^\circ$.

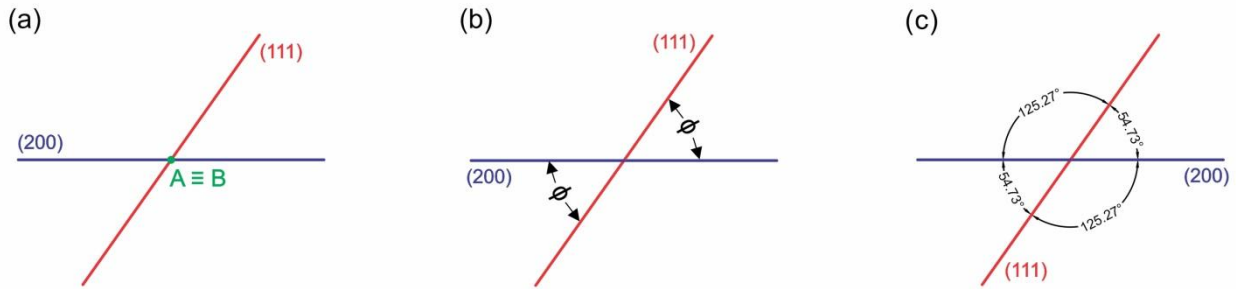


Figure 1 – Point projection of the straight intersection \overline{AB} ($A \equiv B$) and linear projection of planes (111) and (200)

II. MATERIALS AND METHODS

Consulting the crystallographic chart 606003-ICSD [16], where *Al* is described at room temperature (19.85°C), the data set presented in Table 1 were considered.

Table 1 - Main characteristics of the cubic crystalline structure of Al.

Cell Lengths (1×10^{-10} m)	a 4.050(1) b 4.050(1) c 4.050(1)
Cell Angles ($^\circ$)	α 90; β 90; γ 90
Cell Volume (Å^3)	66.43
Space Group	Fm3m (#225) [17]
Temperature ($^\circ\text{C}$)	19.85
<i>Z</i> , <i>Z'</i>	Z : 4 Z' : 0
Density (CCDC)	2.7

Each *Al* atom has a coordination number of 12 ($\text{CN} = 12$), as shown in Figure 2(a) and Figure 2(b). In addition, the crystal contains 14 atoms distributed in a face-centered cubic structure (FCC), as shown in Figure 2(c). According to Figure 2(d), each one of this 14 atoms coordinates with other 12 neighboring atoms. This 3D visualization was made using the software Mercury 4.3.0 USA, under license.

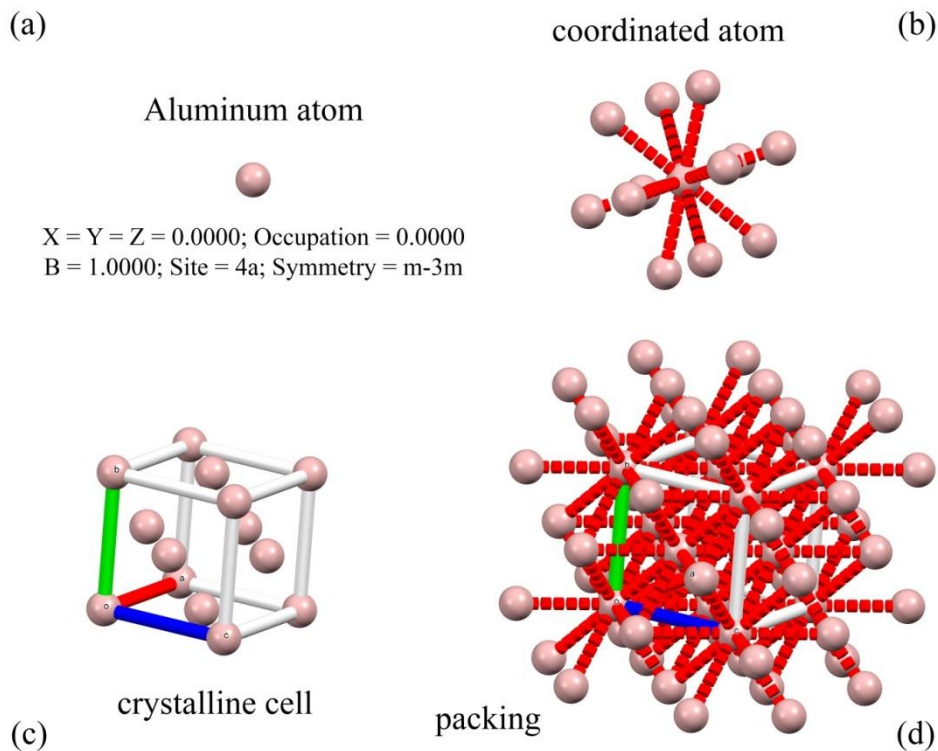


Figure 2 – Primary structuring of long-range crystalline packaging.

Each numbered atom (1-14) has a position in relation to the origin 0,0,0 on the respective X,Y,Z axes. In addition, it is noted, as shown in Table 2, that each of them has a unique symmetry operator. There are therefore, 4 whole atoms per cubic crystalline cell. Hence, the atomic packing factor (APF) is equal to 0,74, i.e.the relationship between the volume of atoms within the unit cell and the volume of the unit cell, also known as volumetric density, represents 74 % of this cube[18].

Table 2–Individual position of atoms in the crystal and their respective symmetry operators.

Number	Label	Charge	SybylType	Xfrac + ESD	Yfrac + ESD	Zfrac + ESD	Symm. op.
1	Al1	0	Al	0	0	0	z,y,-x
2				0	0	1	z,y,1-x
3				0	1	0	z,1+y,-x
4				0	1	1	z,1+y,1-x
5				1	0	0	1+z,y,-x
6				1	0	1	1+z,y,1-x
7				1	1	0	1+z,1+y,-x
8				1	1	1	1+z,1+y,1-x
9				0	0.5	0.5	z,1/2+y,1/2-x
10				1	0.5	0.5	1+z,1/2+y,1/2-x
11				0.5	0	0.5	1/2+z,y,1/2-x
12				0.5	1	0.5	1/2+z,1+y,1/2-x
13				0.5	0.5	0	1/2+z,1/2+y,-x
14				0.5	0.5	1	1/2+z,1/2+y,1-x



For the calculation of the ϕ dihedral angle, Equation 02 [26] was adopted. As the network parameters are the same ($a = b = c = 4.050 \text{ \AA}$), this dimension was not considered. However, for the non-cubic structures, the same methodological sequence as described here is followed.

$$\cos\phi = \frac{h_1 \cdot h_2 + k_1 \cdot k_2 + l_1 \cdot l_2}{\sqrt{(h_1^2 + k_1^2 + l_1^2) \cdot (h_2^2 + k_2^2 + l_2^2)}} \quad (02)$$

In this work, Equation 03, was established with a diminutive effect, for the calculation of the angular difference $\varphi [^\circ]$ that exists between the largest angle ($2\theta_{max(hkl)}$) reflected (between Bragg positions) and each one individually: $2\theta_{i(hkl)}$. The last difference will always be equal to zero.

$$\varphi = 2\theta_{max(hkl)} - 2\theta_{i(hkl)} \quad (03)$$

III. RESULTS AND DISCUSSIONS

The indexation of the diffracted peaks was the preliminary step for preparing the necessary data to calculate ϕ angles in neighboring pairs of planes (h k l). In addition, in Table 3, other variables that are important in the process of detailing the diffractometric profile are related to such crystalline planes.

Table 3 – Values calculated from the crystallographic chart: Miller indices (h k l), interplanar distance d, structure factors F, Bragg positions $2\theta_{hkl} (^\circ)$, percent intensity *Int* and Multiplicity.

h	k	l	d (Å)	F(real)	F(imag.)	F	$2\theta [^\circ]$	Intensity %	Multiplicity
1	1	1	2.338269	34.995732	0.938377	35.0083	38.4684	100	8
2	0	0	2.025000	32.778655	0.924183	32.7917	44.71609	47.00982	6
2	2	0	1.431891	26.668206	0.869522	26.6824	65.08939	26.7154	12
3	1	1	1.221121	23.240310	0.830659	23.2552	78.21995	28.37073	24
2	2	2	1.169134	22.227407	0.818094	22.2425	82.42605	7.98894	8
4	0	0	1.012500	18.693810	0.769708	18.7096	99.06718	3.71259	6
3	3	1	0.929134	16.500617	0.735306	16.5170	112.00213	12.58682	24
4	2	0	0.905608	15.843153	0.724184	15.8597	116.55076	12.33487	24
4	2	2	0.826703	13.527063	0.681352	13.5442	137.42469	13.95746	24
3	3	3	0.779423	12.071827	0.650899	12.0894	162.44679	9.70399	8
5	1	1	0.779423	12.071827	0.650899	12.0894	162.44679	29.11196	24
4	4	0	0.715946	10.072278	0.603138	10.0903	-1, #IND0	-1, #IND0	12

The angular values of Phi (ϕ) were calculated and the respective results, presented in Table 4, showed that the data set are derived from a population considered statistically normal, since the resulting p-value is equal to 0.4987 [27], i.e. greater than the 0.05 significance level. Therefore, it is not possible to reject normality. This indicates that the sample analyzed has a high degree of relative crystallinity. The 2D graph of Shapiro-Wilk normalities are presented in the appendices (Figure 7).

Table 4 – Final results found for the ϕ angle in each of the 11 pairs of crystalline planes.

Planes (indexes)		Intersections	Cos ϕ	arc cos ϕ	Angle ϕ [$^{\circ}$]	angular difference φ
1 $^{\circ}$	2 $^{\circ}$					
111	200	1	0.5774	0.9553	54.7356	123.97839
200	220	2	0.7071	0.7854	45.0000	117.7307
220	311	3	0.8528	0.5495	31.4822	97.3574
311	222	4	0.8704	0.5148	29.4962	84.22684
222	400	5	0.5774	0.9553	54.7356	80.02074
400	331	6	0.6882	0.8117	46.5085	63.37961
331	420	7	0.9234	0.3940	22.5746	50.44466
420	422	8	0.9129	0.4205	24.0948	45.89603
422	333	9	0.9428	0.3398	19.4712	25.0221
333	511	10	0.7778	0.6797	38.9424	0
511	440	11	0.8165	0.6155	35.2644	0

Figure 4(a) and Figure 4(b) demonstrate the individual behavior of the first two crystalline planes reported [$2\theta = 38.46^{\circ}$ (111) and $2\theta = 44.71^{\circ}$ (200)], in addition to the intersection between them represented in perspective in Figure 4(c). The point projection of the straight intersection determines four angles. Each pair of planes opposed by the vertex have congruent (equal) angles. The smallest sum of these angular openings represents the dihedral angles ϕ .

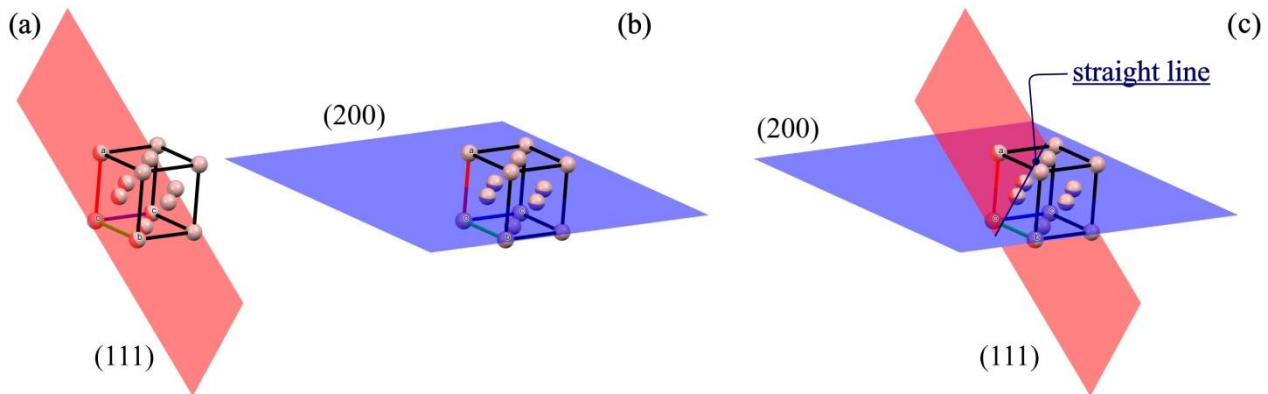


Figure 4 – Individual presentation and intersection of the first 2 crystalline planes studied: (111) e (200)

As shown in Figure 5, the values found for φ confirmed the decreasing correlation of this variable with the value of the dihedral angle ϕ . The determination coefficient found ($R^2 = 0.9846$) measures the quality of the fit of the linear regression and expresses, above all, the extent to which both variables are related to each other.

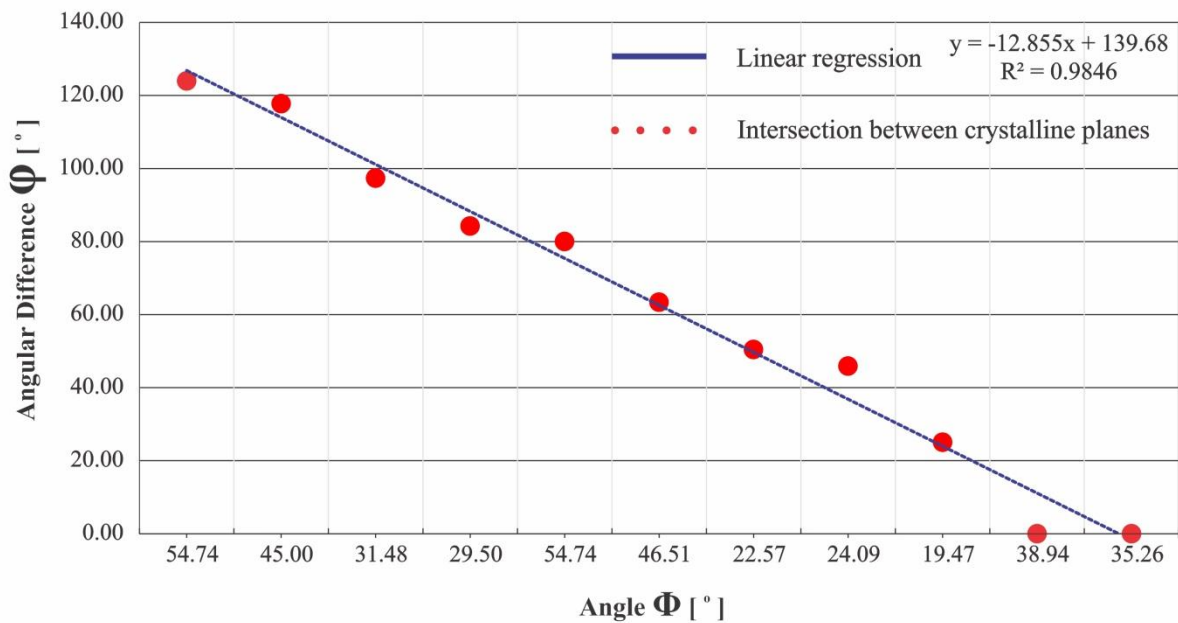


Figure 5 – Linear relationship between dihedral angles ϕ and the typical angular difference ϕ .

IV. CONCLUSIONS

The results obtained in this study point to the following statements:

- The ϕ angles calculated are limited to the following statistical measures: Mean: 36.57323 °; Standard Deviation: 12.47776 °; SE of mean: 3.76219°; Lower 95% CI of Mean: 28.19055°; Upper 95% CI of Mean: 44.9559°; Variance: 155.69446; Sum: 402.3055°; Skewness: 0.21378; Kurtosis: -1.26381; Uncorrected Sum of Squares: 16270.55513°; Corrected Sum of Squares: 1556.94464°; Coefficient of Variation: 0.34117; Mode: 54.7356°.
- Quantiles can be grouped with the following values: Minimum: 19.4712 °; 1st Quartile (Q1): 24.0948 °; Median: 35.2644 °; 3rd Quartile (Q3): 46.5085 °; Maximum: 54.7356 °; Interquartile Range (Q3 - Q1): 22.4137 °; Range (Maximum - Minimum): 35.2644 °; Median Absolute Deviation: 11.1696 °; Robust Coefficient of Variation: 0.4696.
- Of the 11 ϕ angles considered, only 2 of them are greater than 45°. Thus, 81,81 % of them are less than 45 °. This indicates a clear trend in the predominance of every sharp dihedral angles ($90 > \phi < 45$).
- It is also possible to use this same methodology for polyphasic materials, simply separating the positions of Bragg [2 θ] that refers to a certain phase, separating it from the other phases. In this case, if there are 3 hypothetical phases, there will be three separate plotted graphs, similar to what happens with a single phase in Figure 5.

ACKNOWLEDGMENT

Authors would like to acknowledge CAPES - Coordination for the Improvement of Higher Education Personnel; The databases from BDEC (Crystalline Structure Database): ASM Materials Information, Cambridge Structural Database System (CSDS), CrystMet and Inorganic Crystal Structure Database (ICSD). The Federal University of Campina Grande (UFCG); the Mechanical Engineering Department at UFCG; the Multidisciplinary Laboratory for Materials and Active Structures (LaMMEA); the Academic Unit of Mechanical Engineering (UAEMec); the Materials Characterization Laboratory (LCM - UAEMec); the Academic Unit of Production Engineering (UAEP); and to the Science and Technology Center (CCT-UFCG).

REFERENCES

1. Cullity, B., *Elements of X-ray Diffraction*. Addison and Wesley Publishing Company Inc. Reading, USA, 1978: p. 32-106.
2. Richardson, M.J. and N.L. Balazs, *On the network model of molecules and solids*. Annals of Physics, 1972. **73**(2): p. 308-325.
3. Groom, C.R., et al., *{The Cambridge Structural Database}*. Acta Crystallographica Section B, 2016. **72**(2): p. 171--179.
4. Hall, S.R. and R. Sievers, *CIF applications. I. QUASAR: for extracting data from a CIF*. Journal of Applied Crystallography, 1993. **26**(3): p. 469-473.
5. Suryanarayana, C. and M.G. Norton, *X-ray diffraction: a practical approach*. 2013: Springer Science & Business Media.
6. Frank, F., *On Miller–Bravais indices and four-dimensional vectors*. Acta Crystallographica, 1965. **18**(5): p. 862-866.
7. Momma, K. and F. Izumi, *VESTA 3 for three-dimensional visualization of crystal, volumetric and morphology data*. Journal of Applied Crystallography, 2011. **44**(6): p. 1272-1276.
8. Downs, R.T. and M. Hall-Wallace, *The American Mineralogist crystal structure database*. American Mineralogist, 2003. **88**(1): p. 247-250.
9. Palmer, D.C., *Visualization and analysis of crystal structures using CrystalMaker software*. Zeitschrift für Kristallographie-Crystalline Materials, 2015. **230**(9-10): p. 559-572.
10. Chichagov, A., et al., *MINCRYST: A crystallographic database for minerals, local and network (WWW) versions*. Crystallography Reports, 2001. **46**(5): p. 876-879.
11. Finger, L.W., M. Kroeker, and B.H. Toby, *DRAWxtl, an open-source computer program to produce crystal structure drawings*. Journal of Applied Crystallography, 2007. **40**(1): p. 188-192.
12. Sharma, M. and D. Mishra, *CrysX: crystallographic tools for the Android platform*. Journal of Applied Crystallography, 2019. **52**(6): p. 1449-1454.
13. Pennington, W.T., *DIAMOND—visual crystal structure information system*. Journal of Applied Crystallography, 1999. **32**(5): p. 1028-1029.
14. Bergerhoff, G., M. Berndt, and K. Brandenburg, *Evaluation of Crystallographic Data with the Program DIAMOND*. Journal of research of the National Institute of Standards and Technology, 1996. **101**(3): p. 221-225.
15. Ultra, C., *6.0 and Chem3D Ultra*. Cambridge Soft Corporation, Cambridge, USA, 2001.
16. Kokot, L., R. Horyn, and N. Iliew, *The niobium-aluminium binary system phase equilibria at 1100 °C and superconductivity of alloys*. Journal of the Less Common Metals, 1976. **44**: p. 215-219.
17. Breneman, G.L., *Crystallographic symmetry point group notation flow chart*. Journal of Chemical Education, 1987. **64**(3): p. 216.
18. Callister Jr, W.D. and D.G. Rethwisch, *Fundamentals of materials science and engineering: an integrated approach*. 2012: John Wiley & Sons.
19. Authier, A., *Dynamical theory of X-ray diffraction*. International Tables for Crystallography, 2006: p. 626-646.
20. Shapiro, S.S. and M.B. Wilk, *An analysis of variance test for normality (complete samples)*. Biometrika, 1965. **52**(3/4): p. 591-611.
21. Lilliefors, H.W., *On the Kolmogorov-Smirnov test for normality with mean and variance unknown*. Journal of the American statistical Association, 1967. **62**(318): p. 399-402.
22. Abdi, H. and P. Molin, *Lilliefors/Van Soest's test of normality*. Encyclopedia of measurement and statistics, 2007: p. 540-544.
23. Scholz, F.W. and M.A. Stephens, *K-sample Anderson–Darling tests*. Journal of the American Statistical Association, 1987. **82**(399): p. 918-924.
24. Ahmad, M. and A. Al-Mutairi, *Journal of ISOSS 2017 Vol. 3 (1), 35-44 NORMALITY TESTS: A BRIEF REVIEW*. Journal of ISOSS, 2017. **3**(1): p. 35-44.
25. Bai, Z. and L. Chen, *Weighted W test for normality and asymptotics a revisit of Chen–Shapiro test for normality*. Journal of statistical planning and inference, 2003. **113**(2): p. 485-503.
26. Brandon, D. and W.D. Kaplan, *Microstructural characterization of materials*. 2013: John Wiley & Sons.
27. Royston, P., *Approximating the Shapiro-Wilk W-test for non-normality*. Statistics and computing, 1992. **2**(3): p. 117-119.

APPENDICES

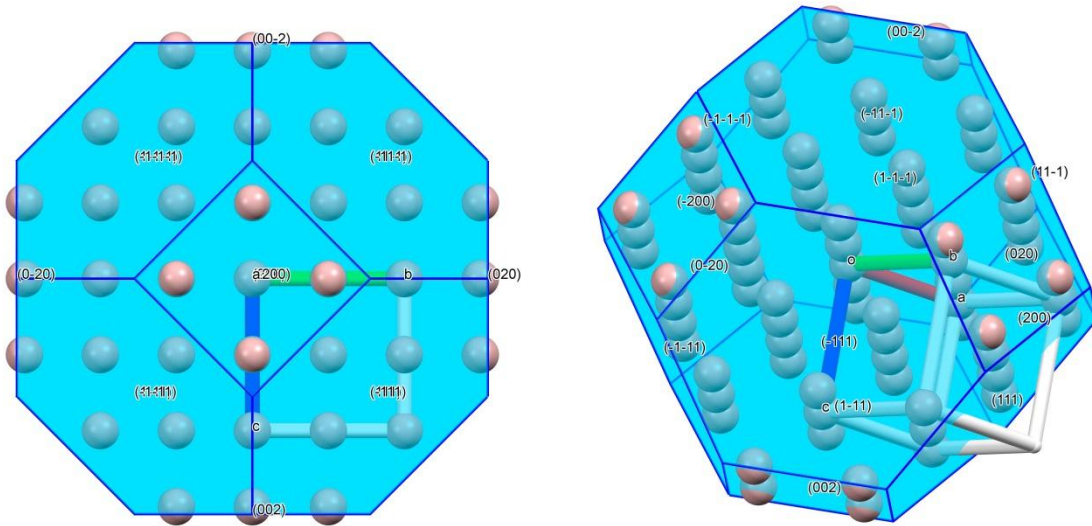


Figure 6 – Orthographic views and perspective of the truncated octahedron which contains the family of crystallographic planes.

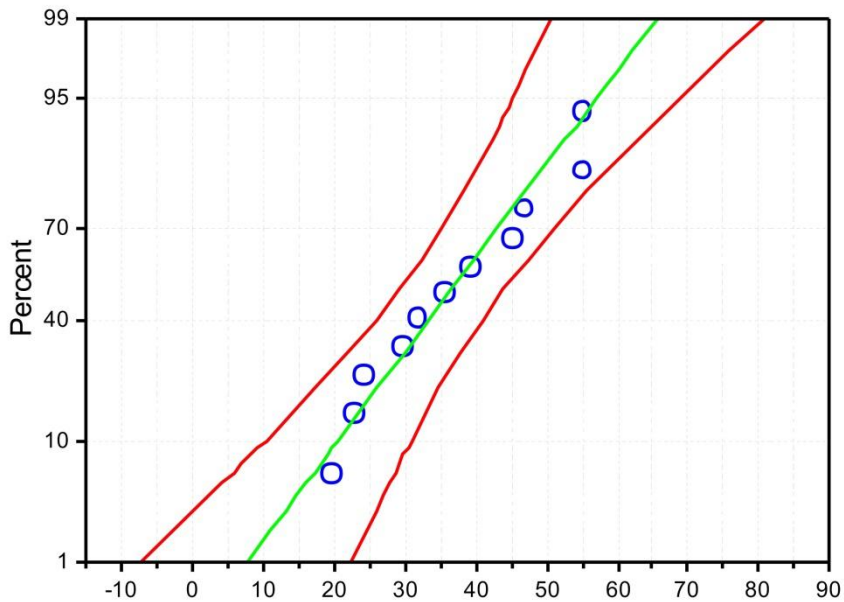


Figure 7 - Probability Plot of Column Angle ϕ . Normal \rightarrow $\mu = 36.57323$; $\sigma = 12.47776$; $\alpha = 0.05$ [S-W]. DF = 11; Statistic = 0.93813106912165; p-value = 0.49878227792259; Decision at level (5%); Can't reject normality; At the 0.05 level, the data was significantly drawn from a normally distributed population.

BIOGRAPHIES



Roniere Leite Soares – Was born in Campina Grande, Paraíba State, Brazil, in 1972. Is an Adjunct Professor at the Federal University of Campina Grande-PB (UFCG), based in the Academic Unit of Production Engineering, Graphic Expression Area, T-40 full time contract. Is graduated in Industrial Design from the Federal University of Paraíba (UFPB, 1991-1995) and has a degree in Letters, from the State University of Paraíba (UEPB, 1997-2003). Has an interdisciplinary master's degree in Society Sciences (UEPB, 2003-2005) and master's in Materials Science and Engineering (UFCG, 2011-2013), where developed a redesign of the Bellouard microvalve. Holds a doctorate degree from the Postgraduate Program in Materials Science and Engineering (UFCG, 2015-2019), where developed intelligent de Ni-Ti-Hf materials. <http://lattes.cnpq.br/0494374289705105>



Walman Benício de Castro – Is graduate in Mechanical Engineering from the Federal University of Paraíba (UFPB, 1988), has a master's in Mechanical Engineering (Campina Grande-PB) from UFPB (1992) and a doctorate in Materials Science and Engineering from the Federal University of São Carlos (1997). Currently, is a Full Professor at the Federal University of Campina Grande. Has experience in materials and metallurgical engineering, with emphasis on casting and solidification, acting mainly on the following themes: supercooling, microstructure, fast solidification, shape-memory alloys and electromagnetic microsystems. Is a professor of the Postgraduate Program in Materials Science and Engineering (PPGCEMat) at the UFCG. <http://lattes.cnpq.br/3592569966434979>



Jackson de Brito Simões – Was born in Campina Grande, Paraíba State, Brazil, in 1982. Is graduate in Business from the State University of Paraíba (UEPB, 2006); graduate in Mechanical Engineering from the Federal University of Campina Grande (UFCG, 2006), holds a master's degree in Mechanical Engineering (UFCG, 2012) and doctorate in Materials Science and Engineering (UFCG, 2016). Has experience in mechanical engineering, with emphasis in mechanical projects and materials and manufacturing processes, acting mainly on the following topics: shape-memory alloys, advanced materials, smart materials, development and applications of shape-memory alloys, manufacturing, simulation and development of metallurgical processes. Is a professor at the Federal Rural University of the Semi-Arid (UFERSA). <http://lattes.cnpq.br/8279861117114431>



Raiff Leite Soares – Was born in Campina Grande, Paraíba State, Brazil, in 1977. Holds a bachelor's degree in Physiotherapy from the State University of Paraíba (2003). Graduated in Medicine at the Federal University of Campina Grande (2014), medical residency in Orthopedics and Traumatology at the State Hospital for Emergency and Trauma Senador Humberto Lucena, João Pessoa-PB (2018). Is also a specialist in Shoulder and Elbow Surgery and Arthroscopy at the Institute of Traumatology and Orthopedics Romeu Krause (ITORK). Is a full member of the Brazilian Society of Orthopedics and Traumatology (SBOT). Is a specialist in Orthopedics and Traumatology from the (SBOT, 2018) and in Traumatology-Orthopedic Physiotherapy from the University Gama Filho, Rio de Janeiro-RJ (2004). Lately, has had great personal interest in the area of materials science and engineering because of the use of metals and alloys in orthoses and rehabilitation prostheses. <http://lattes.cnpq.br/3021504930348781>